Journal of Alloys and Compounds 501 (2010) 233–235

Contents lists available at ScienceDirect

Journal of Alloys and Compounds

journal homepage: www.elsevier.com/locate/jallcom

Rate capability of spinel $LiCr_{0.1}Ni_{0.4}Mn_{1.5}O_4$

G.Q. Liu[a,*], L. Wen[b], G.Y. Liu[a], Y.W. Tian[a]

[a] School of Material and Metallurgy, Northeastern University, Shenyang 110004, China
[b] Chinese Acad Sci, Inst Met Res, Shenyang Natl Lab Mat Sci, Shenyang 110016, China

ARTICLE INFO

Article history:
Received 3 March 2010
Received in revised form 27 March 2010
Accepted 1 April 2010
Available online 20 April 2010

Keywords:
$LiCr_{0.1}Ni_{0.4}Mn_{1.5}O_4$
Li-ion batteries
Cathode material
Properties
Rate capability

ABSTRACT

The spinel compound $LiCr_{0.1}Ni_{0.4}Mn_{1.5}O_4$ is synthesized by a sol–gel method. In this synthesizing process, $Li(CH_3COO)\cdot 2H_2O$, $Ni(CH_3COO)_2\cdot 4H_2O$, $Mn(CH_3COO)_2\cdot 4H_2O$ and $Cr(NO_3)_3\cdot 9H_2O$ are used as reactants, and malic acid as chelating agent. The reaction takes place at 900 °C for 8 h. The electrochemical performances of the as-prepared sample are measured at different current rates. In the range of 3.5–5.0 V, its discharge capacities are 141, 125 and 95 mAh g^{-1} at 0.5, 1 and 5 C, respectively. Based on cycle voltammetry results, the diffusion coefficient of Li^+ is calculated as 6.75×10^{-10} cm^2 s^{-1} at 4.07 V in oxidation process.

1. Introduction

In recent years, the spinel material $LiNi_{0.5}Mn_{1.5}O_4$ has attracted much attention because of its advantages of low cost, low toxicity and good electrochemical performances. The most remarkable property of spinel $LiNi_{0.5}Mn_{1.5}O_4$ is its higher discharge plateau at around 5.0 V. The high working voltage can lead to a high power density, so the batteries with this material as cathode will produce a high power output. Nevertheless, the cycling stability of the LNMO-based cathodes at high rates is not satisfactory.

The structural and electrochemical properties of the $LiNi_{0.5}Mn_{1.5}O_4$ could also be affected by the substitution of other metal ions. Cation doping is considered to be an effective way to modify the intrinsic properties of electrode materials. It will be promising if proper cation doping can be used in spinel $LiNi_{0.5}Mn_{1.5}O_4$ to further improve its electrical conductivity, favoring fast charge and discharge rate. So far, some researches related to elements have been reported, such as doping Al [1], Fe [2], Cu [3], Co [4,5], Ti [6–8], Cr [9–13], Mg [14,15] and Ru [16]. These doping elements had different influences on improving the electrochemical properties of $LiNi_{0.5}Mn_{1.5}O_4$. Until now the spinel $LiNi_{0.5}Mn_{1.5}O_4$ with trace Ru-doping has been reported to exhibit the best electrochemical properties, including rate capability and cyclic performance. Wang et al. [16] reported that $Li_{1.1}Ni_{0.35}Ru_{0.05}Mn_{1.5}O_4$ and $LiNi_{0.4}Ru_{0.05}Mn_{1.5}O_4$ could deliver discharge capacities of 108 and 117 mAh g^{-1} at 10 C between 3 and 5 V, respectively. At 10 C, they could maintain 91% and 84% of their initial capacities after 500 cycles, respectively. Because the price of Ru is high, Ru-doped materials will be costly.

In this study, we doped $LiNi_{0.5}Mn_{1.5}O_4$ with small amount of Cr by a sol–gel method in which malic acid was used as chelating agent. The rate capability of doped compound $LiCr_{0.1}Ni_{0.4}Mn_{1.5}O_4$ was measured at different charge–discharge current densities. The lithium diffusion coefficient was also measured from the relationship between scan rates and peak current of cyclic voltammogram.

2. Experimental

To prepare $LiCr_{0.1}Ni_{0.4}Mn_{1.5}O_4$ material, a sol–gel method was employed. Stoichiometric amounts of $Li(CH_3COO)\cdot 2H_2O$, $Ni(CH_3COO)_2\cdot 4H_2O$, $Mn(CH_3COO)_2\cdot 4H_2O$ and $Cr(NO_3)_3\cdot 9H_2O$ were used as starting materials and malic acid as chelating agent. In order to compensate for the loss of Li at high reaction temperature, approximate additional 3% of Li salt was made up. At first, the staring materials were dissolved in distilled water and stirred for some time, and then added malic acid into aqueous solution drop by drop. After stirred for 2 h, the mixed solution was evaporated at 80 °C to form a dried gel. At last, the gel was calcined at 900 °C for 8 h to turn into product.

Chemical analysis of the synthesized materials was performed with an inductively coupled plasma-atomic emission spectrometer (ICP-AES, Optima 4300DV, PE Co. Ltd.). Based on the analysis results, the chemical formula of the products was determined.

The phase identification of the prepared samples was carried out by X-ray diffraction (XRD) using a Multiflex X-ray powder diffractometer (Rigaku Co. Ltd.). X-ray profiles were measured between 10° and 90° (2θ angle) with a monochromatic Cu Kα radiation source. The morphologies of the products were examined with a JEOL JSM-5600LV scanning electron microscope (SEM).

The electrochemical properties of the products were tested in cells with metallic lithium as anode electrode. The cathode was separated from the Li anode by a layer of celgard 2300 membrane soaked with the electrolyte of 1 M $LiPF_6$ in a 1:1 (v/v)

* Corresponding author. Tel.: +86 024 83673860; fax: +86 024 83687731.
E-mail address: liugq@smm.neu.edu.cn (G.Q. Liu).

0925-8388/$ – see front matter © 2010 Elsevier B.V. All rights reserved.
doi:10.1016/j.jallcom.2010.04.076

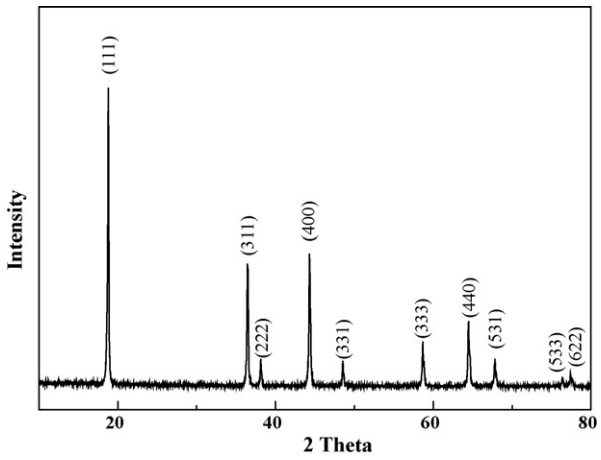

Fig. 1. X-ray diffraction (XRD) patterns for $LiCr_{0.1}Ni_{0.4}Mn_{1.5}O_4$.

mixture of ethylene carbonate (EC) and dimethyl carbonate (DMC). The cathode was prepared by blade-coating a slurry of 90% (weight percent) active material, 5% conducting carbon black, and 5% PVDF binder in NMP on an aluminum foil, drying in an oven, roller-pressing and dried coated foil, and punching out circular discs of 1.23 cm^2. The active material of cathode weighed 8.5 mg, and it was 20 um thick. The cells were assembled in an argon-filled dry box. Charge–discharge tests were performed at a constant current density, in the range of 3.5–5.0 V. All the tests were carried out at room temperature.

Cycle voltammetry (CV) was carried out at room temperature by using the above cells. CV was conducted at a scan rate of 0.05 mV/s between 3.5 and 5.0 V versus Li/Li^+.

3. Results and discussion

The product was analyzed by ICP, and the result indicated that the ratio of Ni:Mn:Cr:O was approximately 0.4:1.5:0.1:4, respectively. Fig. 1 shows the XRD patterns of the prepared $LiCr_{0.1}Ni_{0.4}Mn_{1.5}O_4$.

It also can be seen that there are no peaks at 37.5°, 43.6° and 63.3° in the pattern, illustrating that there were no secondary phases NiO and $Li_xNi_{1-x}O$ [17]. The pure phase compound $LiCr_{0.1}Ni_{0.4}Mn_{1.5}O_4$ was obtained. Spinel $LiNi_{0.5}Mn_{1.5}O_4$ has two possible structures of face-centered spinel (*Fd3m*) and primitive simple cubic crystal ($P4_332$). For $LiNi_{0.5}Mn_{1.5}O_4$ with a face-centered structure (*Fd3m*), the lithium ions are located in the 8a sites of the structure, the manganese and nickel ions are randomly distributed in the 16d sites. The oxygen ions which are cubic-close-packed (ccp) occupy the 32e positions. For $LiNi_{0.5}Mn_{1.5}O_4$ ($P4_332$) with a primitive simple cubic structure, the manganese ions are distributed in 12d sites, and nickel ions in 4a sites. The oxygen ions occupy the 24e and 8c positions, while the lithium ions are located in the 8c sites. In this case, the Ni and Mn ions are ordered regularly [18]. Because these two structures differ very little, it is difficult to distinguish them from XRD patterns. However, in the *Fd3m* space group, there are both Mn^{3+} and Mn^{4+}, while in the $P4_332$ space group, all Mn ions are Mn^{4+} [19]. The voltage plateau at about 4 V resulted from Mn^{3+}/Mn^{4+} in the subsequent charge–discharge curves indicates the presence of Mn^{3+}. So it can be inferred that the product $LiCr_{0.1}Ni_{0.4}Mn_{1.5}O_4$ has a cubic spinel structure with *Fd3m* space group.

The micrograph of $LiCr_{0.1}Ni_{0.4}Mn_{1.5}O_4$ sample is shown in Fig. 2. The product exhibited polyhedral shapes. The particle sizes distribute unevenly, ranging from 0.2 to 5 μm.

The charge–discharge properties of $LiCr_{0.1}Ni_{0.4}Mn_{1.5}O_4$ at different current rates of 0.5, 1 and 5 C are shown in Fig. 3. In order to avoid polarization of electrode, electrolyte must be infiltrated into active materials. So several hours are needed for this infiltrating process before the measuring is done. It has been clarified by the

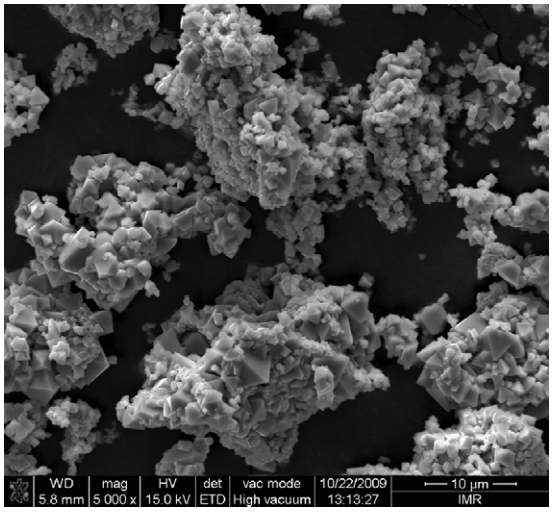

Fig. 2. Scanning electron micrograph of the pure phase $LiCr_{0.1}Ni_{0.4}Mn_{1.5}O_4$.

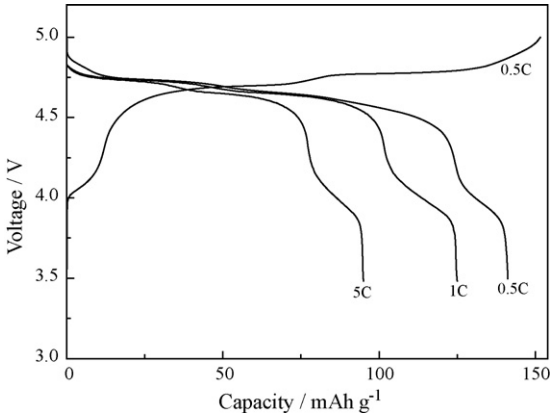

Fig. 3. Charge/discharge curves for $LiCr_{0.1}Ni_{0.4}Mn_{1.5}O_4$ between 3.5 and 5.0 V at current rates of 0.5, 1 and 5 C.

previous research that the electrochemical process taking place at around 4 V involves the oxidation of Mn^{3+} to Mn^{4+}, while the two plateaus above 4.5 V are caused by Ni^{2+}/Ni^{3+} and Ni^{3+}/Ni^{4+} transitions. The first discharge capacities at 0.5, 1 and 5 C were 141, 125 and 95 mAh g^{-1}, respectively.

The differential chronopotentiometry tests (d*Q*/d*V*) were also carried out, and its result is shown in Fig. 4. Two oxidation

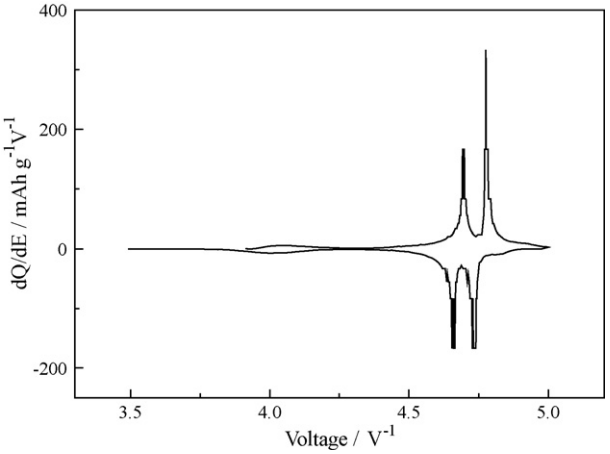

Fig. 4. Differential chronopotentiograms for $LiCr_{0.1}Ni_{0.4}Mn_{1.5}O_4$.

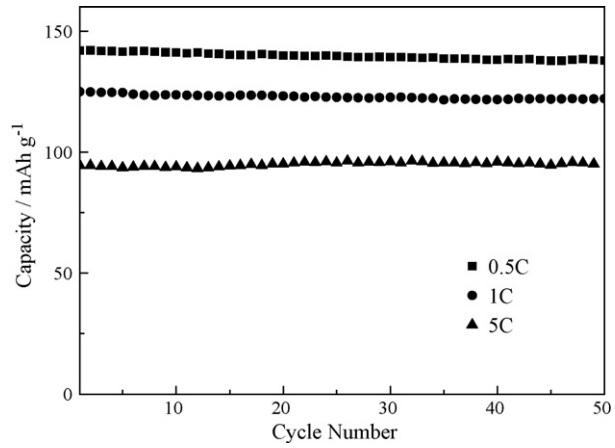

Fig. 5. Cycle performances of $LiCr_{0.1}Ni_{0.4}Mn_{1.5}O_4$ at different current rate.

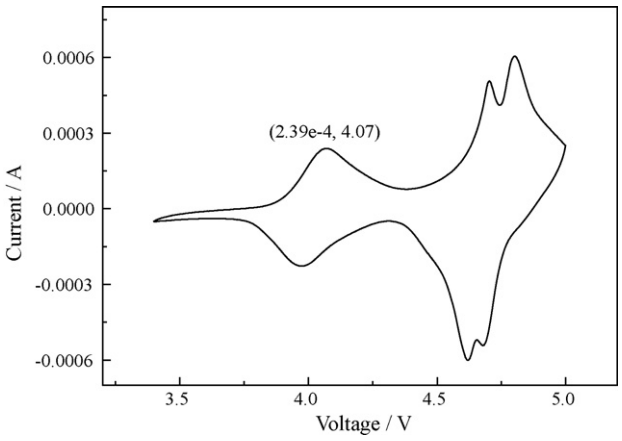

Fig. 6. Cyclic voltammogram of $LiCr_{0.1}Ni_{0.4}Mn_{1.5}O_4$.

peaks at 4.69 and 4.78 V and the corresponding reduction peaks at 4.65 and 4.73 V were observed. There was also a small oxidation–reduction peak at 4.0 V, corresponding to the small plateau of the charge–discharge curve. The peak at 4.69 V is due to the oxidation/reduction of Ni^{3+}/Ni^{2+} and the peak at 4.78 V is due to the oxidation/reduction of Ni^{4+}/Ni^{3+}.

Fig. 5 shows the cycle performance of $LiCr_{0.1}Ni_{0.4}Mn_{1.5}O_4$ at the current density of 0.5, 1 and 5 C. After 50 cycles, the capacity retentions remained well at the different current rates. This result demonstrates that the as-prepared $LiCr_{0.1}Ni_{0.4}Mn_{1.5}O_4$ had good cycle performance. As the cycle proceeded, larger current rates resulted in polarization which caused the capacity to decline. The polarization was related to the low ion conducting rate of electrolyte and migration of Li ion in the cathode lattice and anode structure.

Fig. 6 shows the CV curves of $LiCr_{0.1}Ni_{0.4}Mn_{1.5}O_4$. Three redox processes are clearly seen in CV curves. The redox processes include Mn^{3+}/Mn^{4+}, Ni^{2+}/Ni^{3+} and Ni^{3+}/Ni^{4+}. They take place at around 4.07, 4.70 and 4.80 V, respectively, which is in accordance with the above charge–discharge and differential chronopotentiometry test results. Based on the following equation [20], the diffusion coefficient of Li^+ in the electrode can be calculated.

$$I_p = (2.65 \times 10^5) n^{3/2} S D_{Li}^{1/2} C_{Li} \nu^{1/2}$$

where I_p, the peak current density is in A cm^{-2}, D_{Li} is in $cm^2\ s^{-1}$, S measured in cm^2, D_{Li} in $cm^2\ s^{-1}$, C_{Li} in mol cm^{-3}, and ν in V s^{-1}. Substituting experimental data into this equation, we can get diffusion coefficient of Li ion, i.e., $D_{Li} = 6.75 \times 10^{-10}\ cm^2\ s^{-1}$.

These experimental results indicate that partial replacement of Ni in $LiNi_{0.5}Mn_{1.5}O_4$ with Cr is an effective one to improve its rate capability because the bonding energy of Cr–O is stronger than that of Mn–O and Ni–O. The stronger Cr–O bond is in favor of maintaining the spinel structure during cycling. This prevents the structural disintegration of the material.

It should be pointed out that the $LiCr_{0.2}Ni_{0.4}Mn_{1.4}O_4$ exhibited better the rate capability at different discharge rates and same charge rate of 0.5 C [13]. However, in this manuscript, the charge and discharge tests were carried out at same rates. The particle sizes of $LiCr_{0.2}Ni_{0.4}Mn_{1.4}O_4$ are also smaller than those of $LiCr_{0.1}Ni_{0.4}Mn_{1.5}O_4$. Small particles have advantages for lithium batteries. The advantages include short path lengths for Li^+ transport, short path lengths for electronic transport, higher electrode/electrolyte contact area leading to higher charge/discharge rates. Therefore, it should not indicate that rate performance of the $LiCr_{0.1}Ni_{0.4}Mn_{1.5}O_4$ is inferior to the $LiCr_{0.2}Ni_{0.4}Mn_{1.4}O_4$. In addition, the specific capacity of doped $LiNi_{0.5}Mn_{1.5}O_4$ is affected by doping element. For the Cr doped $LiMn_{1.5}Ni_{0.5}O_4$, the more amount of Cr element is doped, the less capacity at around 4.7 V will be obtained theoretically. So the 0.1 doping amount is an optimal value for the Cr doped $LiMn_{1.5}Ni_{0.5}O_4$.

4. Conclusion

A simple sol–gel method was used to synthesize spinel compound $LiCr_{0.1}Ni_{0.4}Mn_{1.5}O_4$ in this study. The as-prepared product had a cubic spinel structure with *Fd3m* space group. It exhibited good rate capacity. It could deliver discharge capacities of 141, 125 and 95 mAh g^{-1} at 0.5, 1 and 5 C, respectively, with good capacity retention. At 4.07 V in oxidation process, the diffusion coefficient of Li^+ was calculated as $6.75 \times 10^{-10}\ cm^2\ s^{-1}$ according to cycle voltammetry test results.

References

[1] S.H. Yang, R.L. Middaugh, Solid State Ionics 139 (2001) 13.
[2] J. Liu, A. Manthiram, J. Phys. Chem. C 113 (2009) 15073.
[3] Y.E. Eli, J.T. Vaughey, M.M. Thackeray, S. Mukerjee, X.Q. Yang, J. McBreenc, J. Electrochem. Soc. 146 (1999) 908.
[4] R. Alcantara, M. Jaraba, P. Lavela, J.L. Tirado, J. Electrochem. Soc. 151 (2004) A53.
[5] A. Ito, D. Li, Y. Lee, K. Kobayakawa, Y. Sato, J. Power Sources 185 (2008) 1429.
[6] J.H. Kim, S.T. Myung, C.S. Yoon, I.H. Oh, Y.K. Sun, J. Electrochem. Soc. 151 (2004) A1911.
[7] G.Q. Liu, W.S. Yuan, G.Y. Liu, Y.W. Tian, J. Alloys Compd. 484 (2009) 567.
[8] R. Alcantara, M. Jaraba, P. Lavela, J.L. Tirado, P. Biensan, J.P. Peres, Chem. Mater. 15 (2003) 2376.
[9] S.B. Park, W.S. Eom, W. Il Cho, H. Jang, J. Power Sources 159 (2006) 679.
[10] M. Aklalouchb, J.M. Amarilla, R.M. Roja, I. Saadouneb, J.M. Rojo, J. Power Sources 185 (2008) 501.
[11] K.J. Hong, Y.K. Sun, J. Power Sources 109 (2002) 427.
[12] R.K. Katiyar, R. Singhal, K. Asmar, R. Valentin, R.S. Katiyar, J. Power Sources 194 (2009) 526.
[13] M. Aklalouch, J.M. Amarilla, R.M. Rojas, I. Saadoune, J.M. Rojo, Electrochem. Commun. 12 (2010) 548.
[14] C. Locati, U. Lafont, L. Simonin, F. Ooms, E.M. Kelder, J. Power Sources 174 (2007) 847.
[15] R. Alcantara, M. Jaraba, P. Lavela, Chem. Mater. 16 (2004) 1573.
[16] H.L. Wang, H. Xia, M.O. Lai, L. Lu, Electrochem. Commun. 11 (2009) 1539.
[17] Q. Zhong, A. Bonakdarpour, M. Zhang, Y. Gao, J.R. Dahn, J. Electrochem. Soc. 144 (1997) 205.
[18] N. Amdouni, K. Zaghib, F. Gendron, A. Mauger, C.M. Julien, J. Magn. Magn. Mater. 309 (2007) 100.
[19] J.H. Kim, S.T. Myung, C.S. Yoon, S.G. Kang, Y.-K. Sun, Chem. Mater. 16 (2004) 906.
[20] C.M.A. Brett, A.M.O. Brett, Electrochemistry (Principles, Methods, and Applications), Oxford University Press, 1993, p. 178.